JTTEE5 8:125-132

Study of the Influence of Microstructural Properties on the Sliding-Wear Behavior of HVOF and HVAF Sprayed WC-Cermet Coatings

L. Jacobs, M.M. Hyland, and M. De Bonte

The microstructural properties of WC-Co-Cr and WC-Co coatings deposited by high-velocity oxygen fuel (HVOF) and high-velocity air fuel (HVAF) processes were investigated. The tribological behavior of the coatings was studied by means of pin-on-disk tests. Microcracking of the HVOF sprayed WC-Co coatings did not allow preparation of suitable disks for wear tests. The wear rates of the remaining coatings were determined, and wear tracks on the coatings and counterbodies were investigated by SEM. The HVAF sprayed coatings showed greater sliding-wear resistance compared to the HVOF coatings. The prime wear mechanism in the WC-Co HVAF coatings was adhesive wear. The cobalt matrix is lubricious, resulting in very low wear rates and low debris generation. The main wear mechanisms in the WC-Co-Cr coatings were adhesive and abrasive wear. Adhesive wear results in coating material dislodgments (i.e., "pullouts") that become trapped in the contact zone and act as a third-body abrasive. Particle pullout from the coating significantly increases the wear rate of the coated specimen. The HVAF/WC-Co-Cr coatings exhibited better resistance to particle pullout, resulting in a considerably lower wear rate than the HVOF/WC-Co-Cr coatings.

Keywords HVAF, HVOF, pin-on-disk, sliding wear, WC-cermet coating

1. Introduction

The HVAF system is a high-velocity combustion spray process that uses kerosene and compressed air (not oxygen) for combustion. It was originally developed to reduce the cost of operation, replacing pure oxygen by compressed air, and to increase the flexibility of high-velocity combustion spray processes while retaining the capability to produce superior coatings. Initial studies report that coatings sprayed with the HVAF gun do not show any of the oxidation or decarburization effects that are observed in high-velocity oxygen fuel (HVOF) coatings (Ref 1-3). An earlier study from this laboratory reported on the characterization of WC-10Co4Cr sprayed by HVOF and HVAF, and a WC-12Co sprayed by HVAF alone (Ref 3). To complement this previous work, the WC-12Co was also sprayed by two additional HVOF systems for the study described in this article. This enabled further comparison of HVOF and HVAF coating microstructures, which showed that, unlike HVOF, the HVAF process did not change the chemistry or the microstructure of the investigated WC-cermet powders during spraying; no decomposition or oxidation processes took place during HVAF spraying, resulting in coatings with a 100% retention of WC particles and a complete absence of brittle W_2C. The tribological behavior of these coatings has been investigated to determine how the microstructural differences between HVAF and HVOF coatings influence the wear performance.

L. Jacobs, M.M. Hyland, The University of Auckland, Auckland, New Zealand; **M. De Bonte,** Katholieke Universiteit Leuven, Leuven, Belgium.

2. Materials

Two commercially available WC-cermet powders were sprayed; a WC-Co-Cr "fused and crushed" powder (AMDRY 5843) manufactured by Sulzer-Metco (Wohlen, Switzerland) and a WC-Co CAT (carbide activation technology) powder (WC-616) manufactured by Praxair Specialty Powders (Indianapolis, IN). The powder characteristics are given in Table 1, and the powder morphology is illustrated in Fig. 1.

3. Experimental Procedure

Powders were sprayed onto degreased and grit-blasted steel disks (AISI H13, equivalent to ORVAR1 or DIN 1.2343), 4 mm thick and 60 mm diameter, to a coating thickness of 300 to 400 μm. HVOF spraying of the WC-Co-Cr disks was carried out with a CDS-100 gun (Sulzer Plasma Technik, Wohlen, Switzerland) at the Universitat de Barcelona, Spain, as part of an earlier study on the influence of spray parameters on coating microstructure (Ref 2, 4]. HVOF spraying of the WC-Co disks was

Table 1 Powder characteristics

Powder	Composition	Morphology	Carbon, wt%	Main phases
AMDRY 5843	86%WC-10%Co-4%Cr	Blocky/dense/average to large WC particles	5.3	WC, $(Co,W)_6C$
WC-616	88%WC-12%Co	Spherical/porous/small WC particles	5.0	WC, Co

performed at the Thermal Spray Laboratory of the State University of New York at Stony Brook, using a Hybrid Diamond Jet 2700 (DJ-2700) gun (Sulzer Metco, Wohlen, Switzerland) and a HV-2000 gun (Praxair Surface Technologies, Appleton, WI, USA). HVAF spraying was conducted with an Aerospray gun (Browning Thermal Systems Inc., Enfield, NH, USA) at Holster Engineering, New Zealand. The spray parameters are summarized in Tables 2 and 3.

After spraying, the coatings were lapped and polished with diamond embedded disks to a nominal thickness of approximately 150 μm. The WC-Co coatings sprayed by HVOF exhibited severe microcracking during lapping, and further investigation of those coatings was therefore abandoned (discussed in section 4). The other coatings did not show this problem and were submitted to pin-on-disk tests.

The coating roughness was evaluated by contactless laser profilometry (Rodenstock RM600); six radial measurements were performed on each disk on sectors with angular spacing of 60°.

Friction and wear tests were performed using a pin-on-disk (POD II) apparatus (MTM, Leuven, Belgium). An inductive friction force (F_x) transducer and an inductive displacement transducer provide on-line measurement of the friction force and the total displacement of the sliding surfaces. A schematic of the POD apparatus is given in Fig. 2. For each coating two disks with three wear tracks per disk were tested, the exception being the WC-Co HVAF coating (1 disk, 3 tracks).

The experiments were performed under ambient conditions. The temperature and the relative humidity varied between 20 and 25 °C and between 45 and 55%, respectively. The load and the linear speed were kept constant at 49 N and 0.46 m/s, respectively. The diameter of the wear track was varied between 28 and

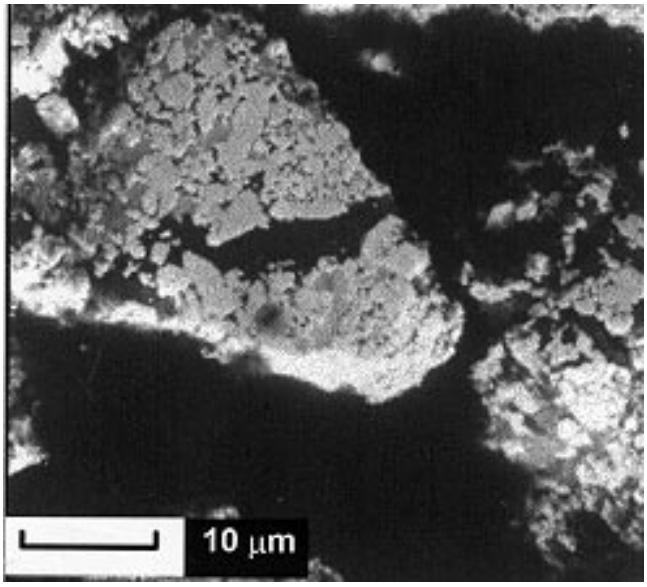

(a)

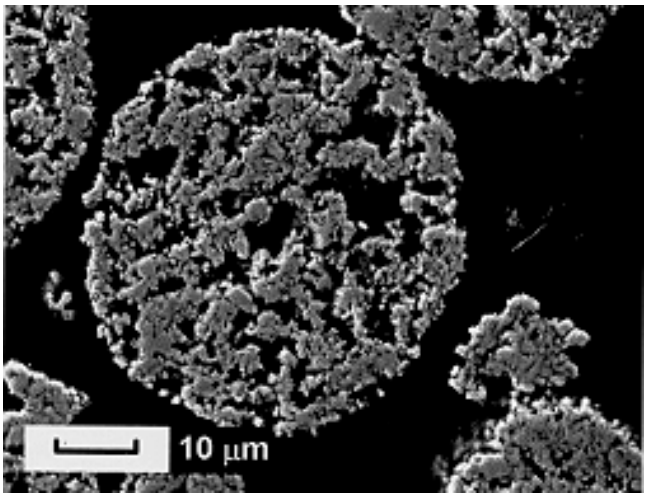

(b)

Fig. 1 SEM micrograph (BSE) of polished cross section of WC-Co-Cr showing the blocky morphology of the "fused-and-crushed" powder. Three phases can be distinguished; WC particles, a light metallic phase rich in cobalt, and a dark metallic phase rich in chromium. (b) SEM image (BSE) showing the spherical morphology and porosity of the WC-Co powder

Table 2 Spray parameters for WC-Co-Cr coatings

	HVOF	HVAF
Gun	CDS-100, Sulzer-Plasma Technik	Aerospray Browning
Combustion mixture	Oxygen: 483 slpm Propane: 63slpm	Air/kerosene, 60 psi
Spray distance, mm	200	200

Table 3 Spray parameters for WC-Co coatings

	HVOF		HVAF
Gun	HV2000, Praxair	Diamond Jet 2700, Sulzer Metco	Aerospray Browning
Combustion mixture	Oxygen: 560 scfh Propylene: 140 scfh	Oxygen: 578 scfh Propylene: 176 scfh	Air/kerosene, 60 psi
Spray distance, mm	250	250	200

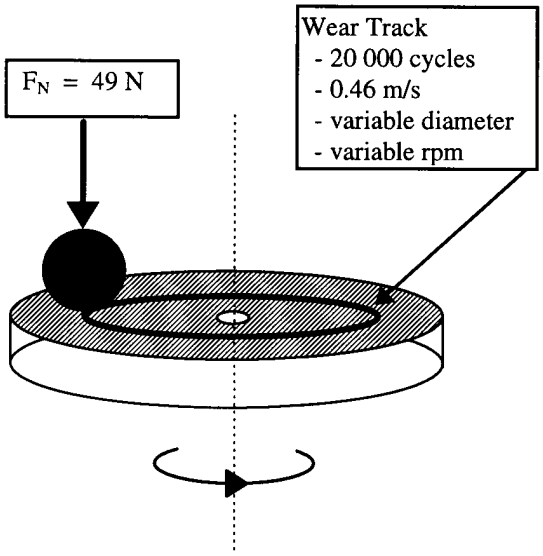

Fig. 2 Schematic of the pin-on-disk apparatus

45 mm, resulting in rotational speeds between 313 and 194 rpm, respectively.

Prior to the tests, the specimens were cleaned with ethanol and dried in hot air. A corundum ball of 10 mm diameter was used as the counterbody. Corundum was selected because of its high coefficient of friction against coatings in dry sliding (Ref 5), which results in accelerated wear. Table 4 shows the properties of the corundum counterbody material. Twenty thousand cycles were performed in each test. After the first 10,000 cycles, the test was stopped and the corundum ball replaced. The test was then resumed, and another 10,000 cycles were performed on the existing wear track. This test procedure also induces accelerated wear.

After the tests, the wear tracks were examined by contactless profilometry. Before the evaluation of the specimen wear volume, the disks were cleaned with water and soap, rinsed in ethanol, and dried in hot air to remove any loose debris. The cross-sectional area (CSA) of the track was obtained from the two-dimensional profiles of the wear track. The average value of the CSA of each wear track was calculated from six measurements along the track. The wear volume of the track was obtained by multiplying the average CSA with the wear track length: $(\pi) \times (WTD)$, with *WTD* the wear track diameter. The wear rate of the coatings was obtained by dividing the wear volume by the total number of cycles and the load (*N*).

The volume loss of the corundum balls was evaluated using a stereomicroscope (WILD Makroskop M 420), which allowed a precise measurement of the diameter of the sphere segment removed during the wear test. From the diameter of the missing sphere segment, the volume loss could be calculated:

$$H = R - \sqrt{R^2 - r^2} \quad \text{(Eq 1)}$$

$$V = \frac{\pi H^2}{3}(3R - H) \quad \text{(Eq 2)}$$

Table 4 Properties of corundum counterbody

Diameter, mm	10
Density, kg/m^3	3800
Weight, g	~2
Average roughness (R_a), μm	~0.04
Hardness, kg/mm^2	2140
Chemical composition, wt%	99.7 Al_2O_3

where *R* is the radius of corundum ball, *r* is the radius of removed sphere segment, *H* is the height of removed sphere segment, and *V* is the volume of removed sphere segment. The wear surfaces of the coatings as well as the counterbodies were characterized using scanning electron microscopy (SEM) coupled with energy dispersive spectroscopy (EDS).

4. Results

4.1 Powder and Coating Characterization

X-ray diffraction (XRD) analysis was performed on the WC-Co-Cr and WC-Co powders as well as on the coatings sprayed by HVAF and HVOF. The powders and coatings all contained WC as the major phase. WC-Co-Cr coatings produced by the HVOF process (CDS-100 gun) show the presence of the W_2C phase as well as the disappearance of the $(Co,W)_6C$ phase that was present in the feedstock powder. The WC-Co coatings sprayed by the two different HVOF processes (DJ-2700 and HV-2000) show the presence of the W_2C and tungsten phases. Relative amounts of these phases are expressed as W_2C-to-WC and W-to-WC peak height ratios in Table 5. These ratios give an indication of the degree of WC decomposition during spraying. The cobalt phase originally present in the WC-Co feedstock powder has been replaced by an amorphous matrix and indicates that decarburization reactions take place due to high-temperature oxidation in flight. Thus, both WC-cermet powders are subject to considerable phase transformation during HVOF spraying. This is in contrast to the HVAF sprayed coatings, where no significant difference between the diffraction pattern of the powder and that of the coatings could be observed, indicating that there is no substantial decarburization or oxidation of the material during HVAF spraying of both WC-cermet powders.

Scanning electron microscopy investigation using backscattered electron imaging of polished cross sections of the coatings confirm the XRD results. As reported previously (Ref 2-4), the WC-Co-Cr HVOF coatings contained blocky WC-particles, somewhat rounded due to oxidation and high-temperature dissolution processes. A binder phase of varying composition was observed: light gray areas contained high percentages of tungsten, darker areas contained more cobalt and/or chromium. In some areas the WC particles have completely disappeared due to these reactions, leaving a tungsten-rich binder phase and W_2C dendrites. W_2C crystals could also be found as very bright halos

Table 5 Coating characteristics

Powder	Process	Carbon, wt%	Main phases	W_2C(a)	W(a)	Microhardness(b) at 100 g, HV	Macrohardness(b) at 1 kg, HV
WC-Co-Cr	HVOF, CDS-100	4.9	WC, W_2C	25.8	0	1220 ± 150(c) 1510 ± 190(d)	900 ± 100
	HVAF, Aerospray	5.3	WC, $(Co,W)_6C$	0	0	1570 ± 290	1050 ± 90
WC-Co	HVOF, DJ-2700	4.11	WC, W_2C, W	13.2	7.5	1200 ± 300	1142 ± 170
	HVOF, HV-2000	3.85	WC, W_2C, W	25.6	8.5	1500 ± 280	801 ± 120
	HVAF, Aeorspray	4.98	WC, Co	0	0	1010 ± 230	700 ± 100

(a) Numbers indicate the ratio of each phase peak height to the d = 1.87Å WC peak height, times 100. This value does not represent a percentage. For W_2C, the d = 2.28 Å peak was used, and for W, d = 2.24 Å. (b) All hardness values are an average of 15 measurements. (c) Hardness measured in metallic region. (d) Hardness measured in region with dispersed carbides (Ref 3)

around the WC particles. The same observations could be made for the HVOF sprayed WC-Co coatings, which are shown in Fig. 3. The HVAF coatings showed a homogeneous distribution of blocky WC particles whose shape was not affected by the spray process. In the case of the WC-Co-Cr HVAF coatings, a binder phase of varying composition was observed, but when compared to the SEM images of the feedstock powder, there was no indication that the binder phase changed composition during spraying (Ref 3). Scanning electron microscopy investigation of the WC-Co HVAF coatings also revealed an unaltered cobalt-binder phase as shown in Fig. 4.

The hardness values of HVOF sprayed WC-Co coatings are significantly higher than the HVAF sprayed analogue, arising from the presence of the hard but brittle W_2C and tungsten phases, also indicative of extensive decarburization during spraying. This brittleness may have been one of the influencing factors for the severe microcracking observed during lapping and polishing of the wear test disks. However, at this stage the precise reason for the microcracking is not fully understood. Other factors such as porosity, residual stresses, and poor splat cohesion might have contributed as well. The HVAF sprayed WC-Co coatings consist of very fine WC particles dispersed in a soft cobalt matrix. This microstructure is less hard, but more ductile, which proves to be beneficial for sliding-wear resistance. A summary of the coating characteristics can be found in Table 5.

4.2 Wear and Friction Performance of the Coatings

The wear data are summarized in Table 6. The last column contains the volume loss of the corundum counterbody. The first value in this column reflects the volume loss during the first 10,000 cycles; the second number gives the volume loss during the next 10,000 cycles. The volume loss of the counterbody was in accordance with the volume loss of the coating; a low wear rate of the coatings was accompanied by a low counterbody wear. Visual examination of the wear tracks after the first 10,000 cycles indicated that little wear had taken place (little wear loss), with most of the wear occurring during the second 10,000 cycles. The volume loss of the counterbody in the first 10,000 cycles was also measurably and consistently lower than in the second cycle set. There is clearly no linear relationship between

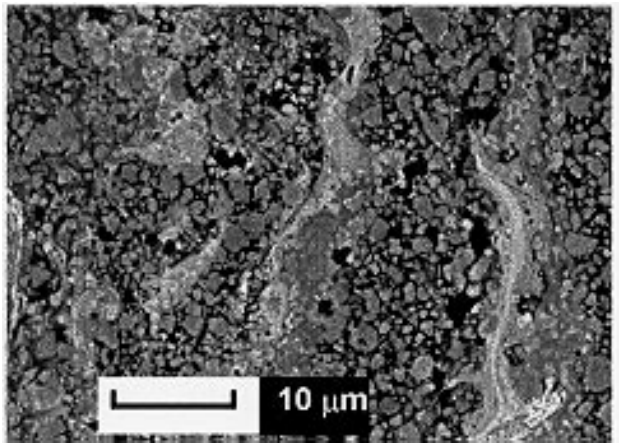

(a)

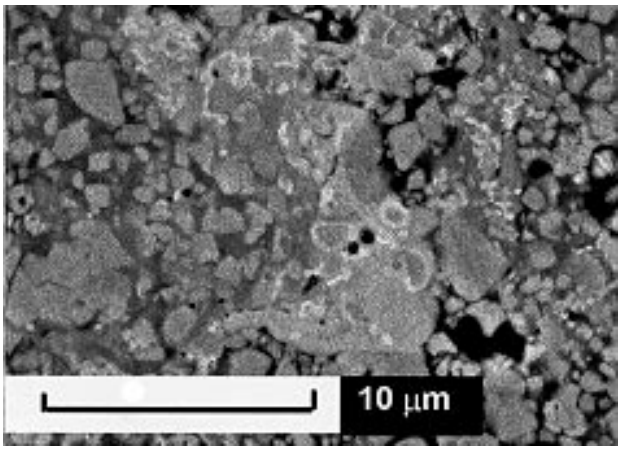

(b)

Fig. 3 (a) and (b) SEM image of WC-Co HVOF coating, sprayed by DJ-2700. There is clear evidence of W_2C halos and dendrites. Note the matrix with a varying composition.

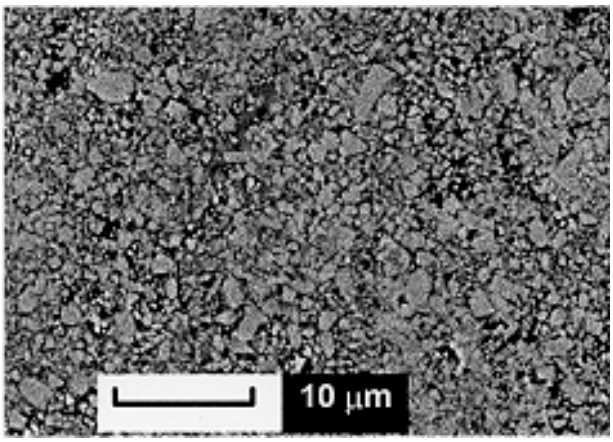

(a)

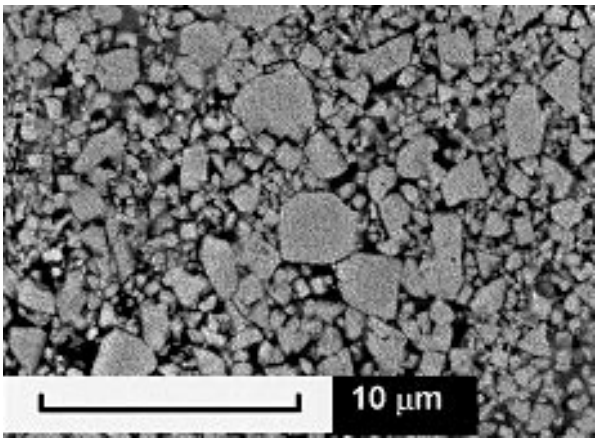

(b)

Fig. 4 (a) and b) SEM image of WC-Co HVAF coating. Note the fine structure of WC particles dispersed in a cobalt matrix. There is no visual sign of W_2C.

wear and the number of cycles. The wear rate, expressed as a volume loss per unit of load and per cycle (Table 6), is thus an average of the two cycles. Therefore, the wear rate obtained in this study might appear higher than in other POD wear studies where the wear rate is generally evaluated in one 10,000-cycle wear test.

4.3 WC-Co-Cr Coatings

Wear Rate. The WC-Co-Cr coatings sprayed by the HVAF process showed wear rates that were an order of magnitude lower and more consistent than those sprayed by HVOF. Visual observations during the wear tests indicated that for the HVAF sprayed WC-Co-Cr coatings abrasive wear was initiated during the second set of 10,000 cycles, while the HVOF sprayed coatings showed abrasive wear during the first set of wear cycles. This suggests that the HVAF coatings were more resistant to pullout, thus initially avoiding three-body abrasive wear. It is worth mentioning here that the HVOF sprayed WC-Co-Cr coatings were optimized for the CDS spray system. This does not suggest, however, that they are the "best" HVOF coatings obtainable, as other HVOF spray techniques might deposit better quality coatings.

Profiles. Figure 5 shows representative wear scar profiles of each coating type as measured by profilometry. The worn HVOF sprayed WC-Co-Cr coatings (C) contain the deepest and widest wear track profiles. The HVAF sprayed WC-Co-Cr coatings (B) show a narrower wear region and a considerable reduction of the wear track depth. In both cases, the wear track is rougher than the initial coating surface, which indicates that particle pullout took place during sliding.

The coefficient of friction (COF) was continuously monitored during the POD tests (Fig. 6). Both WC-Co-Cr coatings display stable frictional behavior with no evidence of a significant increase of friction coefficient after approximately 1000 cycles. The HVOF sprayed WC-Co-Cr coatings rise to a higher COF than the HVAF sprayed WC-Co-Cr coatings, which could be directly related to the initial surface roughness. During the 20,000 cycles for the HVOF coatings, and in the second cycle set for the HVAF coatings, some scatter in the COFs can be observed, indicating that particle pullout is taking place, which supports the visual observations.

Scanning electron microscopy investigation of the morphology of the wear tracks of the HVOF sprayed WC-Co-Cr coatings confirmed that wear primarily arose through particle pullout (Fig. 7a, b). These particles then stayed in the contact area and led to three-body abrasive wear, which was the main wear type in these coatings. The corundum counterbody also shows this form of abrasive wear. There is evidence of severe plowing, with subsequent accumulation of transferred debris in the formed grooves and pores. Some large debris particles could be found adhering to the contact area (Fig. 7c, d). The tracks on the coating and the counterbody were broad, indicating that the coating could not sustain the applied load.

The morphology of the tracks on the HVAF sprayed WC-Co-Cr coatings was not as uniform as the morphology of the HVOF wear tracks. Particle pullout was limited, indicating a better

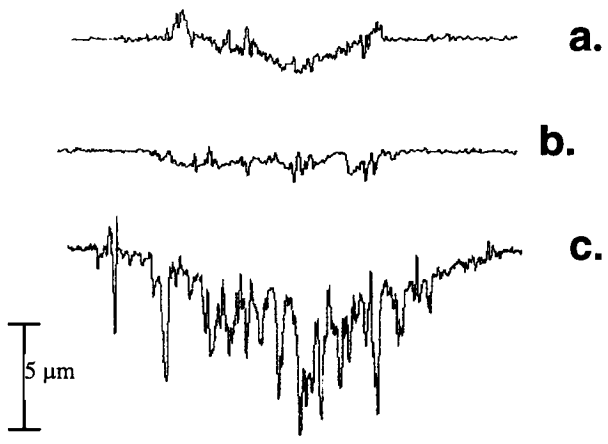

Fig. 5 Representative wear track profiles of (a) HVAF sprayed WC-Co, (b) HVAF sprayed WC-Co-Cr, and (c) HVOF sprayed WC-Co-Cr

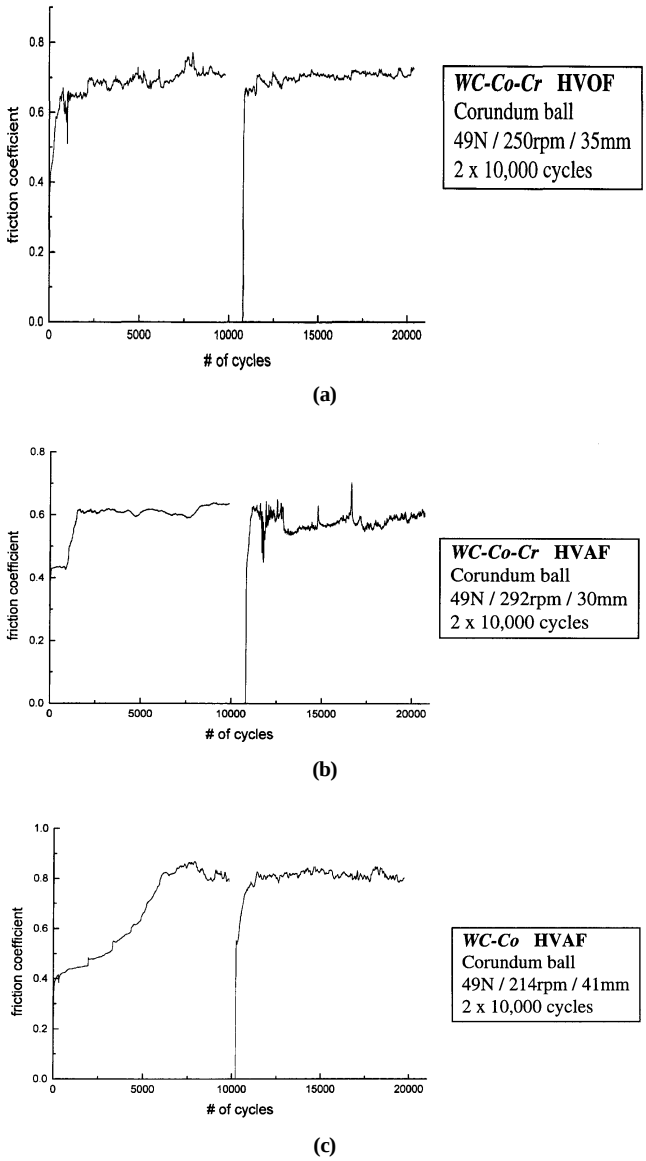

Fig. 6 Evolution of the COF during POD wear tests

coating cohesion and a stronger carbide-matrix interface (Fig. 8a, b). It was clear that particle pullout again eventually initiated three-body abrasive wear (Fig. 8c). The counterbody looks similar to that of the HVOF coatings, although there was less evidence of adhered pullouts and less severe plowing (Fig. 8d, e). The main wear types in this case were still adhesive and abrasive wear, but less pronounced than in the HVOF coatings.

Relationship to Microstructure. The HVAF process, unlike the HVOF process, shows no oxidation or decomposition reactions during spraying (Ref 3). This results in the typical fine and dispersed microstructure of the HVAF coatings, with a phase composition unaltered relative to the spray powder. The HVOF coatings on the other hand are characterized by the presence of brittle W_2C and a brittle binder phase containing high concentrations of dissolved tungsten, which seem to contribute to an inferior coating cohesion resulting in increased particle pullout during the wear tests. Previous studies (Ref 5-7) confirm that the abrasion resistance of WC-base coatings is closely related to the degree of chemical degradation. It was concluded that in general, a greater degree of reaction led to a degradation of mechanical properties, including sliding-wear properties. This is in accordance with the findings of this study.

Table 6 Wear data for the unlubricated sliding POD tests, with corundum counterbody, for two sets of 10,000 cycles and a constant load of 49 N

Specimen composition	Surface roughness (R_a), $\mu m \times 10^{-3}$	Testing conditions: linear speed (m/s)/rotational speed (rpm)/diameter (mm)	Cross-sectional area (CSA), $\mu m^2 \times 10^3$	Wear rate, 10^{-6} mm/cycle · N	Volume loss of counterbody [first counterbody] + [second counterbody], mm^3
WC-Co-Cr,	28 ± 6	0.458/194/45	1.6 ± 0.2	0.23 ± 0.03	[0.1600] + [0.3900]
HVOF CDS-100,		0.458/250/35	6.3 ± 0.6	0.71 ± 0.07	[0.2300] + [0.6200]
disk 1		0.458/313/28	4.0 ± 0.6	0.36 ± 0.05	[0.2100] + 0.3900]
WC-Co-Cr,	27 ± 6	0.458/194/45	1.0 ± 0.1	0.14 ± 0.01	[0.1300] + [0.2800]
HVOF CDS-100,		0.458/250/35	4.0 ± 0.5	0.45 ± 0.06	[0.1600] + [0.3900]
disk 2		0.458/313/28	4.8 ± 0.5	0.43 ± 0.04	[0.1600] + [0.4500]
WC-Co-Cr,	17 ± 4	0.458/194/45	0.44 ± 0.02	0.063 ± 0.003	[0.0013] + [0.0640]
HVAF Aerospray,		0.458/250/35	0.22 ± 0.02(a)	0.025 ± 0.002	[No loss] + [0.0013]
Disk 1		0.458/292/30	0.77 ± 0.05	0.075 ± 0.005	[0.0024] + [0.0720]
WC-Co-Cr,	14 ± 1	0.458/194/45	0.4 ± 0.1	0.05 ± 0.01	[0.0013] + [0.0640]
HVAF Aerospray,		0.458/250/35	0.77 ± 0.02	0.087 ± 0.002	[0.0640] + [0.0830]
Disk 2		0.458/292/30	0.6 ± 0.1	0.056 ± 0.009	[0.0490] + [0.0720]
WC-Co,	18 ± 3	0.458/194/45	0.24 ± 0.05	0.035 ± 0.007	[0.0006] + [0.0203]
HVAF Aerospray		0.458/250/35	0.20 ± 0.04	0.022 ± 0.004	[0.0006] + [0.0063]
		0.458/214/41	0.25 ± 0.05	0.032 ± 0.007	[0.0040] + [0.0203]

(a) No abrasive wear, only polishing wear

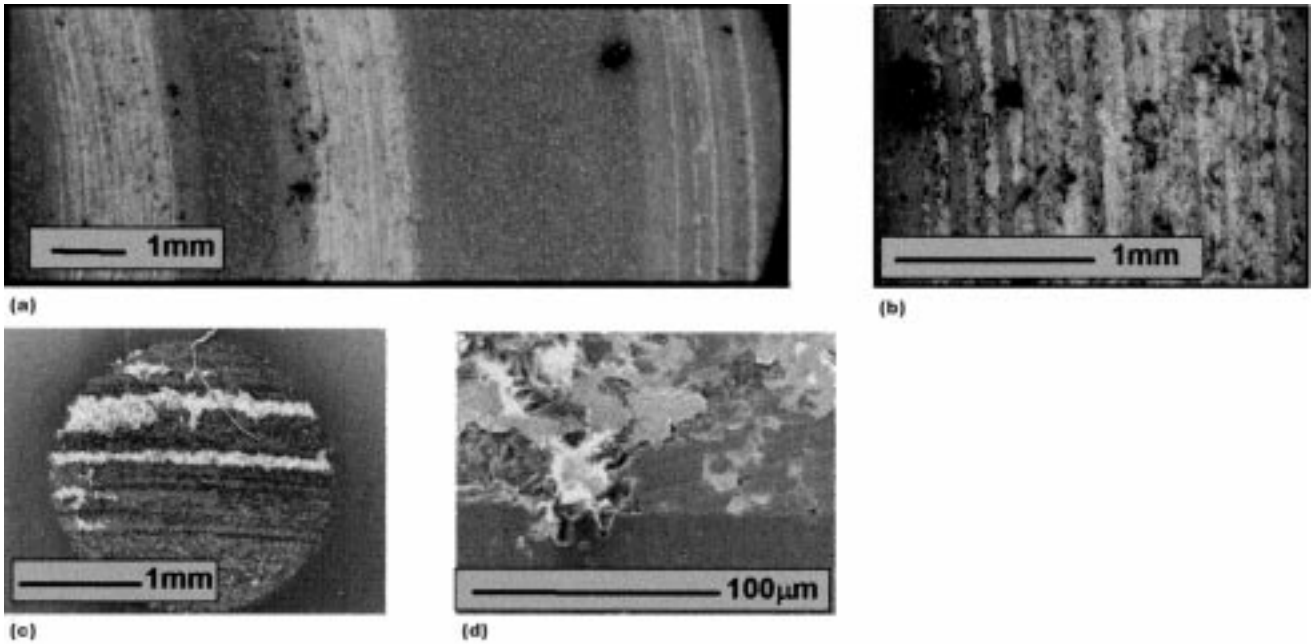

Fig. 7 Wear system investigation. POD testing of the HVOF, WC-Co-Cr coating against corundum, at 49 N and 0.46 m/s. (a) Morphology of the wear track on the coating. (b) High magnification of an area on the track. (c) Contact surface of the corundum counterbody with evidence of plowing and adhesion of large pullout particles transferred from the coating. (d) Transferred material filling up the pores of the corundum counterbody

4.4 WC-Co

The best sliding-wear resistance of all tested coatings is shown by the HVAF sprayed WC-Co coating. This coating shows reproducible, low wear rates (Table 6). The coating shows a narrow and smooth wear track profile (Fig. 5). The smoothness of the track and the obvious material build-up at the edges of the wear track indicate that a different wear mechanism is active compared to the WC-Co-Cr coatings. The COF of the WC-Co coating increased steadily from 0.4 to 0.8 over approximately 7000 cycles (Fig. 6). From this point on, the COF stayed stable around 0.8, indicative of metal-metal contact rather than ceramic-ceramic or ceramic-metal contact.

Scanning electron microscopy investigation of the morphology of the wear track shows two zones (Fig. 9a, c). The outside of the wear track shows strong macroscopic surface deformation

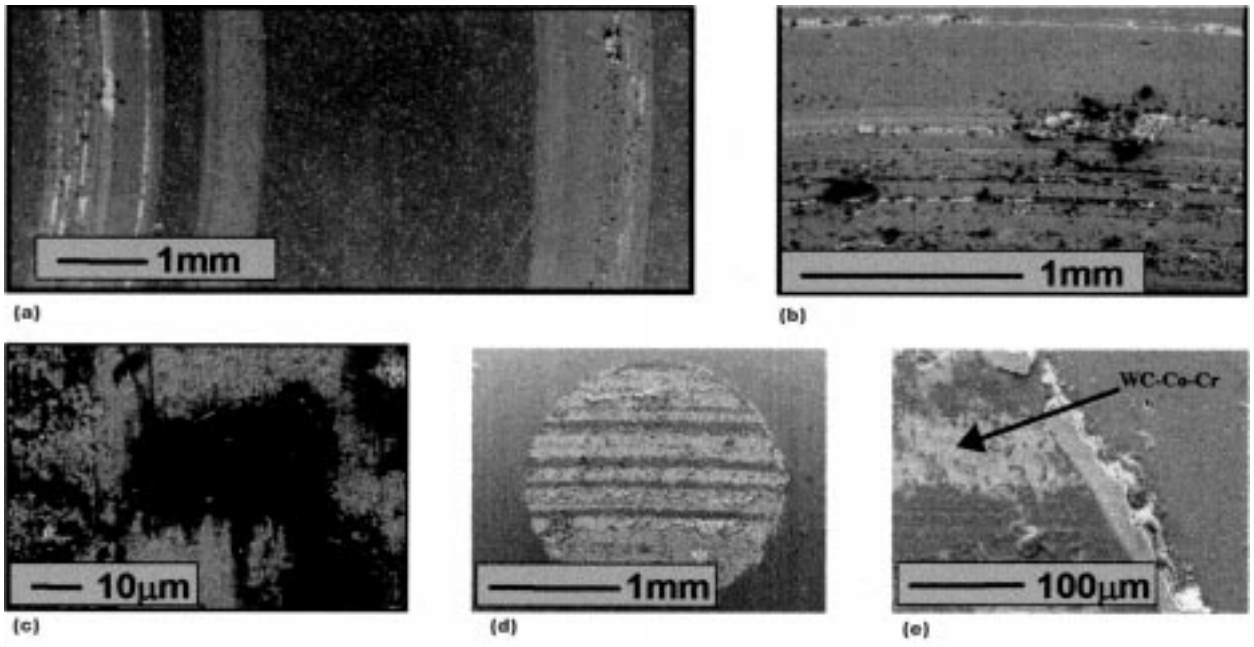

Fig. 8 Wear system investigation. POD testing of the HVAF, WC-Co-Cr coating against corundum, at 49 N and 0.46 m/s. (a) Morphology of the wear track on the coating. (b) High magnification of an area on the track. (c) Evidence of large pullouts (+10 μm) in the wear track of the coating. (d) and (e) Contact surface of the corundum counterbody with evidence of plowing and the accumulation of transferred coating material in the grooves

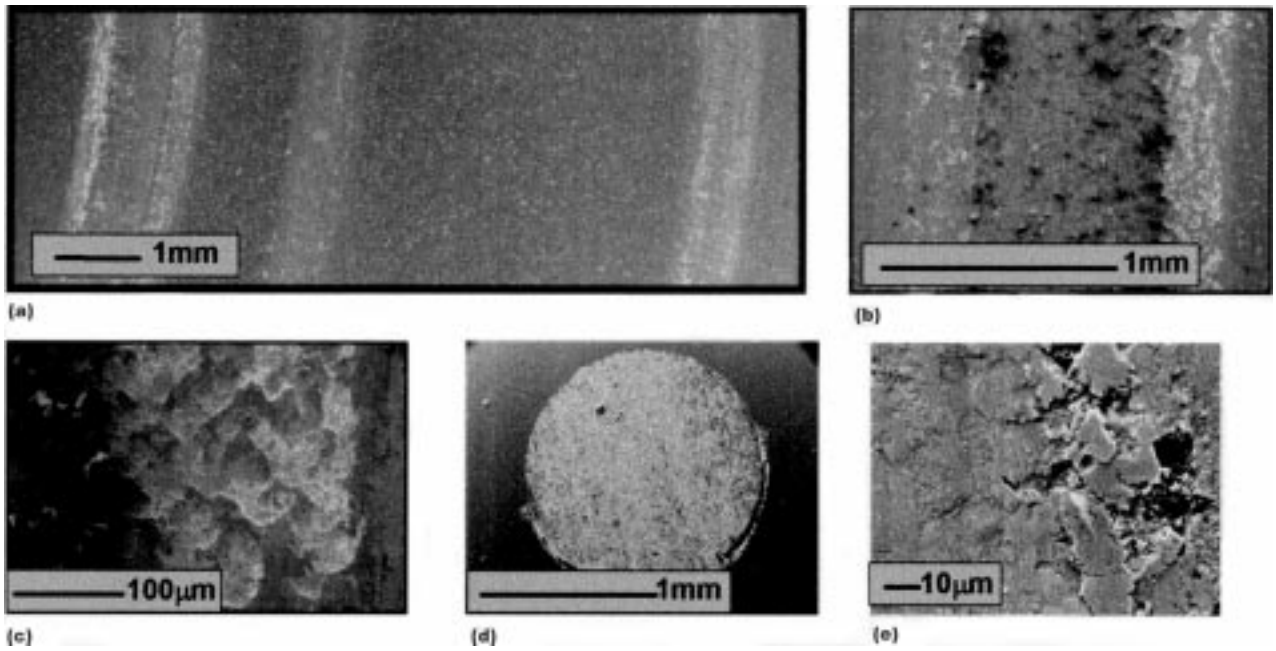

Fig. 9 Wear system investigation. POD testing of the HVAF, WC-Co coating against corundum, at 49 N and 0.46 m/s. (a) Morphology of the wear track on the coating. (b) High magnification of an area on the track where two different wear zones can be distinguished. (c) Detail of the deformed layer at the outside of the wear track. (d) Transferred layer on the contact surface of the corundum counterbody. (e) The transferred layer at high magnification

and some adhesive wear. The middle of the wear track shows very strong adhesive wear resulting in pullouts that are then smeared over the wear track. This explains the low wear rate of this coating and the observation that only a negligible amount of debris was generated during the test. The corundum counterbody is shown in Fig. 9(d, e). Scanning electron microscopy and EDS investigation confirmed that the contact area is entirely covered with a transfer film of smeared debris originating from the coating, which could be expected from the high COF values.

The main wear type here was adhesive wear that did not develop into three-body abrasive wear because of the apparent softness of the binder phase. This caused the coating to deform and the debris to smear over the wear track and caused the contact area of the counterbody to be covered with transferred material. It was shown that a soft binder combined with a homogeneous dispersion of fine WC particles is beneficial for the sliding-wear resistance.

5. Conclusions

The tribological performance of HVOF and HVAF sprayed WC-Co-Cr coatings and a HVAF sprayed WC-Co coating was evaluated in dry sliding against a corundum ball in ambient conditions. Accelerated wear was induced by using a high load of 49 N and by performing two sets of 10,000 cycles with a change of the counterbody after the first 10,000 cycles. Both HVAF coatings showed excellent wear performance.

The main wear types for the HVAF sprayed WC-Co-Cr coatings were three-body abrasive and adhesive wear. During the first 10,000 cycles no particle pullout took place, and very low wear of the coating and the counterbody could be observed. After changing the counterbody, the already damaged wear surface could not sustain the high point load, and subsequent particle pullout induced three-body abrasive wear. This was confirmed by variations in the COF during the second set of 10,000 cycles. The HVOF sprayed WC-Co-Cr coatings showed a wear rate that was an order of magnitude higher than that of the HVAF WC-Co-Cr coatings. Abrasive wear and particle pullout set in immediately after the start of the wear test, resulting in high wear of the coating as well as of the counterbody. The HVAF sprayed WC-Co coating showed the best wear behavior combined with a low wear of the counterbody. The active wear type was adhesive wear. The softness of the binder phase prevented three-body abrasive wear; instead debris of the wear test was smeared over the wear track and over the contact surface of the counterbody.

It could be concluded that the HVAF sprayed coatings that were studied here exhibit an improved sliding-wear performance when compared to the HVOF coatings. This could be explained by the retention of WC particles and the absence of brittle W_2C, which is typical to the HVAF process. The minimization of the decarburization processes during HVAF spraying proves to be advantageous in the deposition of WC-cermet coatings for sliding-wear applications.

Acknowledgment

The authors would like to thank the New Zealand Foundation for Research Science and Technology, who provided the funding. The authors would like to thank Holster Engineering, Tokoroa, New Zealand, for providing HVAF equipment and excellent technical support. The authors wish to acknowledge the research group of Professor Guilemany of the Universitat de Barcelona and the Center for Thermal Spray Research at the State University of New York at Stony Brook, where HVOF spraying was carried out. L. Jacobs acknowledges partial support by the MRSEC program of the U.S. National Science Foundation under contract No. DMR 96-32570 during her stay at SUNY-Stony Brook as a visiting scientist. The authors would also like to thank Praxair Specialty Powders and Sulzer-Metco for providing the spray powders.

References

1. K. Akimoto, K. Akimoto, and Y. Horie, Study of HVAF WC-Cermet Coatings, *Thermal Spray: Current Status and Future Trends*, A. Ohmori, Ed., High Temperature Society of Japan, Osaka, Japan, 1995, p 313-p316
2. L. Jacobs, "Influence of the HVOF Process Conditions on the Structure of WC-Co-Cr Coatings," Master Thesis, Katholieke Universiteit Leuven, 1995 (in Dutch)
3. L. Jacobs, M. Hyland, and M. De Bonte, Comparative Study of WC-Cermet Coatings Sprayed via the HVOF and the HVAF Process, *J. Therm. Spray Technol.*, Vol 7 (No.2), 1998, p 213-219
4. J.M. Guilemany, L. Delaey, F.J. Sanchez, and L. Jacobs, Characterisation of WC + Co + Cr Coatings Obtained by HVOF Spraying, *Metall. Ital.*, Vol 88 (No. 2), 1996, p 133-136
5. S. Economou, "Relationship between Processing, Structure and Tribological Behaviour of Carbide Reinforced Plasma Sprayed Coatings," Ph.D. thesis, Katholieke Universiteit Leuven, Department of Metallurgy and Materials Science Engineering, Belgium, 1995
6. B.R. Marple, J. Voyer, and B. Arsenault, Performance of WC-Based, HVOF Processed Coatings in Sliding Wear, *Thermal Spray: A United Forum for Scientific and Technological Advances*, C.C. Berndt, Ed., ASM International, 1998, p 73-83
7. S.A. Khan and T.W. Clyne, Microstructure and Abrasion Resistance of WC-Co Coatings Produced by High Velocity Oxy-Fuel Spraying, *Thermal Spray: A United Forum for Scientific and Technological Advances*, C.C. Berndt, Ed., ASM International, 1998, p 681-690